

A model filler network in nanocomposites prepared by in situ silica filling and peroxide cross-linking in natural rubber latex

Atitaya Tohsan¹ · Ryota Kishi² · Yuko Ikeda²

Received: 10 November 2014 / Accepted: 25 March 2015 / Published online: 28 April 2015
© Springer-Verlag Berlin Heidelberg 2015

Abstract Preparation and characteristics of model filler networks in nanocomposites are reported for development of rubber science. The nanocomposites were prepared via a sol–gel reaction in natural rubber (NR) latex using tetraethoxysilane followed by a peroxide cross-linking reaction in the liquid state employing a casting method. The filler network structure was formed in the NR matrix, even though the silica content was only 10 and 17 parts per one hundred rubber by weight. One of the important factors for the formation of the filler network was utilization of rubber particles in the latex as a template. Dynamic mechanical analysis revealed the significant characteristics of the filler network of silica particles in the rubber matrix: Higher and longer plateau regions of storage modulus and dissipation loss modulus in the low frequency region were observed in the in situ silica-filled nanocomposites compared with conventionally prepared nanocomposites. This was mainly ascribed to a strong filler–filler interaction.

Keywords Natural rubber latex · In situ silica · Filler network · Peroxide cross-linking · Dynamic mechanical properties

✉ Yuko Ikeda
yuko@kit.ac.jp
Atitaya Tohsan
atitaya@kit.ac.jp

¹ Venture Laboratory, Kyoto Institute of Technology, Matsugasaki, Sakyo, Kyoto 606-8585, Japan

² Graduate School of Science and Technology, Kyoto Institute of Technology, Matsugasaki, Sakyo, Kyoto 606-8585, Japan

Introduction

Natural rubber (NR) is a unique material in rubber technology owing to its outstanding high tensile strength and crack growth resistance after it has been vulcanized. However, it is recognized that the performance of vulcanized NR for many applications can be enhanced by the presence of nanofillers [1–4]. For example, NR/carbon black composites have been exclusively used in heavy duty automobile and aircraft tires. However, carbon black is a product of petroleum, and so its availability may soon decrease because of the eventual limitation of petroleum, which is supposedly near to exhaustion levels. In place of carbon black, particulate silica fillings have been used increasingly in reinforced rubber products because of their characteristic properties, such as transparency [5, 6]. However, it is well known that the dispersion of silica in a rubbery matrix is not as good as that of carbon black because silica has a polar surface, which results in a strong filler–filler interaction that promotes the aggregation of silica particles. This is regarded as one of the reasons for its inferior reinforcement capability.

Using the premise that excellent reinforcement can be achieved when very fine, well-dispersed silica particles are incorporated into a rubbery matrix, in the early 1980s, Mark proposed an in situ sol–gel process using tetraethoxysilane (TEOS) [7]. The Latin “in situ” means “in place,” and therefore, incorporating silica using a sol–gel reaction is considered to be a novel technique. There have been several studies using the sol–gel method to generate in situ silica from alkoxy silane in rubber latexes, including NR latex [8–21]. Recently, we developed a liquid processing technique to fabricate in situ silica/NR latex composites, i.e., dispersed sulfur cross-linking reagents were mixed into a mixture of in situ silica and NR latex, followed by casting and heating to obtain a composite film [19, 20]. As a result, the generated silica was

observed to be locally dispersed around rubber particles to give a filler network. This characteristic morphology conferred good dynamic mechanical properties on the composites. Furthermore, for the first time, the filler network structure of the in situ silica-filled NR composites showed a unique stepwise strain-induced crystallization (SIC) behavior [22]. Pure rubber phases in the filler network were found to afford highly oriented amorphous segments and oriented crystallites upon stretching.

Up to now, a conventional processing technique has been used to prepare a filler network in the nanocomposites. However, the preparation of the model filler network in the rubber matrix has been difficult because a pure rubber phase that is covered by a clear filler network could not be achieved due to formation of various kinds of filler aggregation in rubber matrix. In addition, the conventional milling technique required sufficiently high filler loading in order to reach a so-called “percolation threshold” for forming the network. One of the authors in this study, however, extracted the characteristics of filler networks of carbon black and conventional silica in the rubber matrixes, where a three-dimensional transmission electron microscopy/electron tomography technique (3D-TEM) was utilized [5, 6]. Therefore, the combination of in situ silica filling in the NR latex and solution casting may be a convenient method to produce model nanocomposites providing a filler network for studying on the reinforcement of rubber. The role of the filler network is still an important research topic in rubber science and technology.

To specify clearly the role of the filler network in the rubber matrix, we decided to prepare peroxide cross-linked in situ silica-filled NR composites to avoid the complicated aspects of the sulfur cross-linking reactions of rubber [23, 24]. In this paper, the preparation conditions of peroxide cross-linked in situ silica-filled NR composites are reported, along with the mechanical properties of the resulting nanocomposites. Since a peroxide cross-linking in NR latex has been carried out extensively in the rubber industry for making specific products, the results of this work will prove useful for the rubber industry.

Experimental

Materials

NR latex was ammoniacal latex containing 0.7 % NH_4OH with a dry rubber content (DRC) of 60 %, which was supplied from REGITEX Co., Ltd., Japan. Tetraethoxysilane (Wako Pure Chemical Industries, Ltd., >95 %), tetraethylenepentamine (TEPA; Kanto Chemical Co., Inc. >93 %) and triethoxyvinylsilane (TEVS; Shin-Etsu Chemical Co, Ltd., >99 %) were used as received. A vulcanizing reagent was *t*-butyl hydroperoxide (*t*-BHP; NOF Corporation), which was

mixed with stabilizer [polyoxyethylene lauryl ether (PLE); molecular weight, 1200; Wako Pure Chemical Industries, Ltd., 99 %] in distilled water. Nipsil VN-3 from Nippon Silica Ind. Co., whose specific surface area was around $200 \text{ m}^2/\text{g}$, was used as commercially available silica for the preparation of conventional milled reference samples.

Preparation of peroxide cross-linking NR

Preparation conditions of the peroxide cross-linked films are shown in Table 1, where NR latex with 20 % DRC were used after diluting the commercial NR latex of 60 % DRC using distilled water. TEPA and *t*-BHP, which was dispersed in PLE, were mixed with the NR latex at room temperature (RT) to obtain a uniformly emulsified latex mixture. An unfilled cross-linked NR film was prepared by pouring the latex mixture onto a Teflon mold and followed by heating the mixture at 60, 80, or 100 °C for 0.5, 1, or 2 h, respectively, and drying at RT. Subsequently, the film was dried at 80 °C under a reduced pressure to the constant weight.

Preparation of peroxide cross-linked in situ silica filled NR nanocomposites

Preparation conditions of the nanocomposites are shown in Table 2. The NR latex with 20 % DRC was mixed with TEPA and *t*-BHP, which was dispersed in PLE at RT to obtain a uniformly emulsified latex mixture. Next, the mixture was mixed with TEOS and was kept in an oven at 40 °C for 5 h to progress the sol–gel reaction of TEOS. After the reaction, TEVS was added into the reaction mixture at RT, and the mixture was stirred for 0.5 h at RT. A peroxide cross-linked in situ silica filled NR nanocomposite film was prepared by pouring the mixture onto a Teflon mold and followed by heating the mixture at 80 °C for 0.5 h and drying at RT. Subsequently, it was dried at 80 °C under a reduced pressure to the constant weight.

Thermogravimetry to quantify silica in the nanocomposites

In situ silica contents in the nanocomposites were measured by thermogravimetric analysis (TGA) using a TA instrument TGA2950. The sample was placed in a platinum pan and heated up to 1000 °C at 10 °C/min under air with a flow rate of 60 ml/min. The amount of the sample was around 10 mg. The content was calculated using Eq. (1):

$$\text{Silica content (phr)} = [100W_1/(W_2 - W_1)] - W_3 \quad (1)$$

where W_1 was the weight (mg) of remained ash in the nanocomposite, W_2 was a weight (mg) of nanocomposite, and W_3 was a content in parts per one hundred rubber by weight (phr)

Table 1 Recipe and experimental condition for solution peroxide cross-link in NR latex

Sample code	Surfactant ^a (mg, phr ^b)	<i>t</i> -BHP ^c (mg, phr)	TEPA ^d (mg, phr)	Temperature (°C)	Heating time (h)	$\nu \times 10^4$ (mol/cm ³)
NR-60C-0.5h-0.5p	10.9, 0.075	73, 0.5	55, 0.5	60	0.5	0.8
NR-80C-0.5h-0.5p	10.9, 0.075	73, 0.5	55, 0.5	80	0.5	1.3
NR-100C-0.5h-0.5p	10.9, 0.075	73, 0.5	55, 0.5	100	0.5	1.2
NR-80C-1h-0.5p	10.9, 0.075	73, 0.5	55, 0.5	80	1.0	1.1
NR-80C-2h-0.5p	10.9, 0.075	73, 0.5	55, 0.5	80	2.0	1.2
NR-80C-0.5h-1p	21.7, 0.15	145, 1	110, 1	80	0.5	1.4
NR-80C-0.5h-2p	43.5, 0.3	290, 2	220, 2	80	0.5	1.4

^a Polyoxyethylene lauryl ether

^b Parts per one hundred rubber by weight

^c *t*-Butyl hydroperoxide

^d Tetraethylenepentamine

of remained ash in the unfilled sample (SiO₂), respectively. Note that the residue of the unfilled sample was measured to be 0.06 phr by the TGA measurement.

Observation of morphology by transmission electron microscopy

Morphology of the nanocomposites was observed by transmission electron microscopy (TEM) using a transmission electron microscope (FEI Tecnai G2 F20). The accelerating voltage was 200 kV. The images of TEM were obtained without staining the specimens.

Observation of morphology by scanning probe microscopy

Scanning probe microscopy (SPM) observation was conducted using a Nano-RTM (Pacific Nanotechnology, Inc.) at room temperature. Cantilevers used were NCHR (NanoWorld) whose spring constant and resonance frequency were 42 N/m and 320 kHz, respectively. A phase mode was utilized for the observation, where an image resolution of 512 × 512 points was taken for the samples. The surface of each sample was prepared in liquid N₂ using an MT-XL Ultramicrotome (Boeckeler Instrument, Inc.).

Dynamic mechanical analysis

Time–temperature superposition measurement was conducted using a Rheospectolar DVE-4 instrument. The measurements were performed on as-prepared samples with rectangular geometry having average dimensions of 25 × 5 × 1 mm³. A temperature range was varied from –130 to 150 °C with an increment of 2 °C min^{–1}. Eight data points (frequency=1, 2, 4, 8, 16, 32, 64, and 128 Hz) were taken at each temperature. A tensile mode with dynamic strain ±3 μm and a control strain at 20 % were set for the experiment. Master curves of storage modulus (E'), loss modulus

(E'') and loss tangent ($\tan \delta$) against frequency were constructed using the Williams–Landel–Ferry (WLF) equation [25].

Tensile measurement

Tensile measurement was carried out using a custom-made tensile tester (ISUT-2201, Aiesu Giken Co., Kyoto) at RT. A ring-shaped sample, which has outside and inside diameters 13.7 and 11.7 mm, respectively, was subjected to the tensile measurement in order to correctly measure stretching ratio (α) of the deformed sample. Here, α is defined as $\alpha = l/l_0$, in which l_0 is the initial length and l is the length after deformation. The stretching speed was 100 mm/min, i.e., strain speed was about 4.98 min^{–1}.

Results and discussion

Peroxide cross-linking reaction of NR latex

The effect of the reaction temperature on the peroxide cross-linking of NR was investigated. The reaction temperatures studied were 60, 80, and 100 °C for a reaction time of 0.5 h using the same reagents and surfactants. The network-chain density (ν) was used to compare the reactivity of the peroxide cross-linking of each sample. The value of ν was estimated using the classical theory of rubber elasticity [26].

$$\sigma = \nu RT \left(\alpha - \frac{1}{\alpha^2} \right) \quad (2)$$

where σ is the tensile stress, R is the gas constant, α is the stretching ratio ($\alpha = l/l_0$, where l_0 and l are the initial length and the length after stretching of the sample, respectively), and T is the absolute temperature. The results are shown in Table 1. Among samples NR-60C-0.5h-0.5p, NR-80C-0.5h-0.5p, and NR-100C-0.5h-0.5p, the value of ν for sample NR-80C-0.5h-0.5p was the highest, which suggests that the rate of

Table 2 Recipe for the preparation of peroxide cross-linked nanocomposites samples

Sample	Solution process										Milling process			$\nu \times 10^4$ (mol/cm ³)
	Surfactant ^a (mg, phr ^b)	<i>t</i> -BHP ^c (mg, phr)	TEPA ^d (mg, phr)	TEOS ^e (g, phr)	TEVS ^f (g, phr)	TEOS/TEVS	SiO ₂ (phr)	Film condition	VN3 (phr)	DCP (phr)				
SI0a	21.7, 0.15	145, 1	110, 1	10.2, 35	–	–	N/A	Cracked	–	–	–	2.7		
SI0b	21.7, 0.15	145, 1	110, 1	10.2, 35	10.0, 34.6	1	N/A	Cracked	–	–	–	1.8		
SI0	21.7, 0.15	145, 1	110, 1	–	–	–	0	Good	–	–	–	1.4		
SI10	21.7, 0.15	145, 1	110, 1	10.2, 35	1.0, 3.46	10	10	Good	–	–	–	2.1		
SI17	21.7, 0.15	145, 1	110, 1	20.8, 104	2.1, 10.4	10	17	Good	–	–	–	4.3		
VN20	–	–	–	–	–	–	–	–	20	1	–	2.1		
VN40	–	–	–	–	–	–	–	–	40	1	–	3.7		

^a Polyoxyethylene lauryl ether^b Parts per one hundred rubber by weight^c *t*-Butyl hydroperoxide^d Tetraethylenepentamine^e Tetraethoxysilane^f Triethoxyvinylsilane

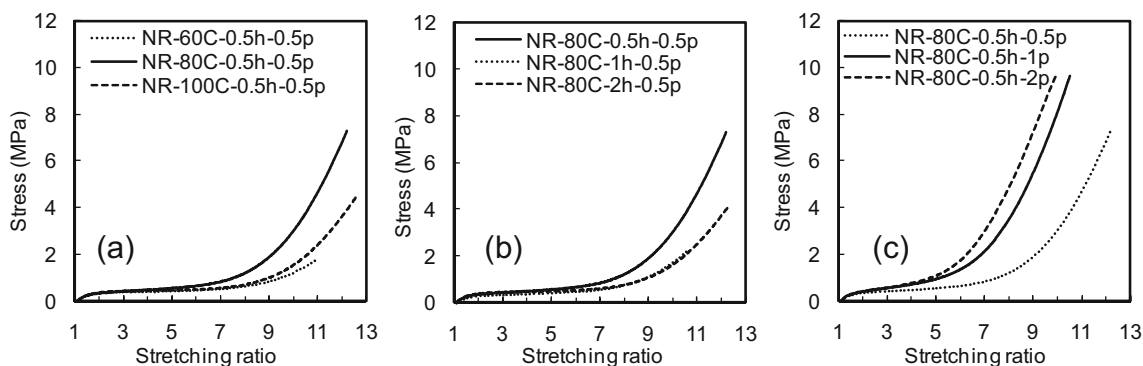


Fig. 1 Tensile stress–strain curves of peroxide cross-linked NR films obtained from NR latex by varying experimental conditions: **a** variation of temperature, **b** variation of time, and **c** variation of amounts of cross-linking reagents

generation of radicals at 60 °C was the lowest, and chain scissions of the NR may have occurred at 100 °C, resulting in the collapse of the network. The results of tensile measurements supported this proposition, as shown in Fig. 1a, where it can be seen that the sample cross-linked at 80 °C showed the highest tensile stress at a stretching ratio >6 among the three samples. Based on these results, a reaction temperature of 80 °C was selected for the preparation of the nanocomposites.

In general, the reaction time of the peroxide cross-linking of rubber is related to the half-life of peroxide, where the half-life is the time required for half of the peroxide to be decomposed at the reaction temperature. It is also well known that the rate of decomposition of peroxide to generate radicals is fastest at the beginning of a reaction, and so a long reaction time is not effective in increasing the degree of cross-linking [27]. Therefore, in this study, three reaction times, i.e., 0.5, 1, and 2 h, were compared at 80 °C. The results for samples NR-80C-0.5h-0.5p, NR-80C-1h-0.5p, and NR-80C-2h-0.5p are summarized in Table 1. The tensile stress–strain curves of the three samples are shown in Fig. 1b. The sample heated at 80 °C for 0.5 h exhibited the highest network-chain density and had the highest tensile stress among the samples. This suggests that, after the reaction time of 0.5 h, almost all the peroxide had decomposed, and only a low concentration remained to continue the reaction. However, when the reaction was allowed to continue for a long time, some cleavage of the NR molecules seems to be occurred [27]. Thus, it was decided to use a cross-linking time of 0.5 h in the preparation of the nanocomposites.

In this study, the peroxide cross-linking reaction of NR latex was processed through a redox reaction, where *t*-BHP, TEPA, and PLE worked as an oxidizing agent, a reducing agent, and a surfactant, respectively [28]. Here, the weight ratio of *t*-BHP/TEPA/PLE was fixed at 1:1:0.15, according to a reference paper [28]. Using this ratio, three different quantities were evaluated to increase the degree of cross-linking of NR in the latex. The results are shown in Table 1, and the tensile stress–strain curves of the samples are shown in Fig. 1c. On increasing the amounts of cross-linking reagents, both the network-chain density and the tensile stress increased. However, it should be

noted that coagulation from the destabilization of the latex was observed for a high cross-linking reagent content, i.e., when 2 phr of *t*-BHP was added to the latex. Thus, the reaction system using 1 phr of *t*-BHP was selected as an appropriate reaction condition at 80 °C for 0.5 h in this study.

Generation of in situ silica in the NR latex

After the optimum conditions for peroxide cross-linking in NR latex were determined, the reaction conditions for the sol–gel reaction of TEOS were subsequently evaluated in the presence of peroxide cross-linking reagents. In Table 2, the results of the sol–gel reaction conditions and film formation are summarized along with the network-chain densities of the samples. When 10.2 g of TEOS was added to the NR latex containing peroxide cross-linking reagents, the resulting nanocomposite, i.e., Si0a did not form a film because of the generation of many cracks in the casting. Cracking during the drying of latex films is usually observed when particles with a glass transition temperature (T_g) above ambient temperature are added to the latex [29, 30]. For example, a similar cracking during drying is commonly observed when adding inorganic (hard) particles, such as alumina and silica, to latex [29, 30]. To overcome the cracking problem observed in this study, a silane-coupling agent, TEVS, was added to the reaction mixture. The TEVS was expected to play the role of a bridge to connect the in situ silica particles with the NR particles in the latex. However, a cracked film was obtained for sample Si0b in the first trial, when 10 g of TEVS was used in a weight ratio of TEOS/TEVS=1:1. This may have been caused by too much TEVS being added. The amount of TEVS added was then reduced to 1 g, where the weight ratio of TEOS/TEVS was 10:1 for sample Si10. In this case, a homogeneous nanocomposite film was obtained. The increase in viscosity of the mixture with no aggregation of silica after adding the TEVS suggests that bonding between the silica particles and the surface of the NR particles in the latex occurred. The combination of TEOS and TEVS was useful in increasing the in situ silica content up to 17 phr. Note that the peroxide cross-linking reaction is supposed to occur partially during the sol–gel reaction at 40 °C because TEPA can

function as a reducing agent at 30 °C to promote the redox reaction in peroxide cross-linking [28]. However, the degree of cross-linking seemed to be low under these conditions because no coagulation was observed during the reaction. Therefore, the reaction solution was heated to 80 °C for 0.5 h after the sol–gel reaction of TEOS at 40 °C for 5 h to cross-link the rubber segments sufficiently. Using this method, both the cross-linking and sol–gel reactions proceeded more or less at the same time.

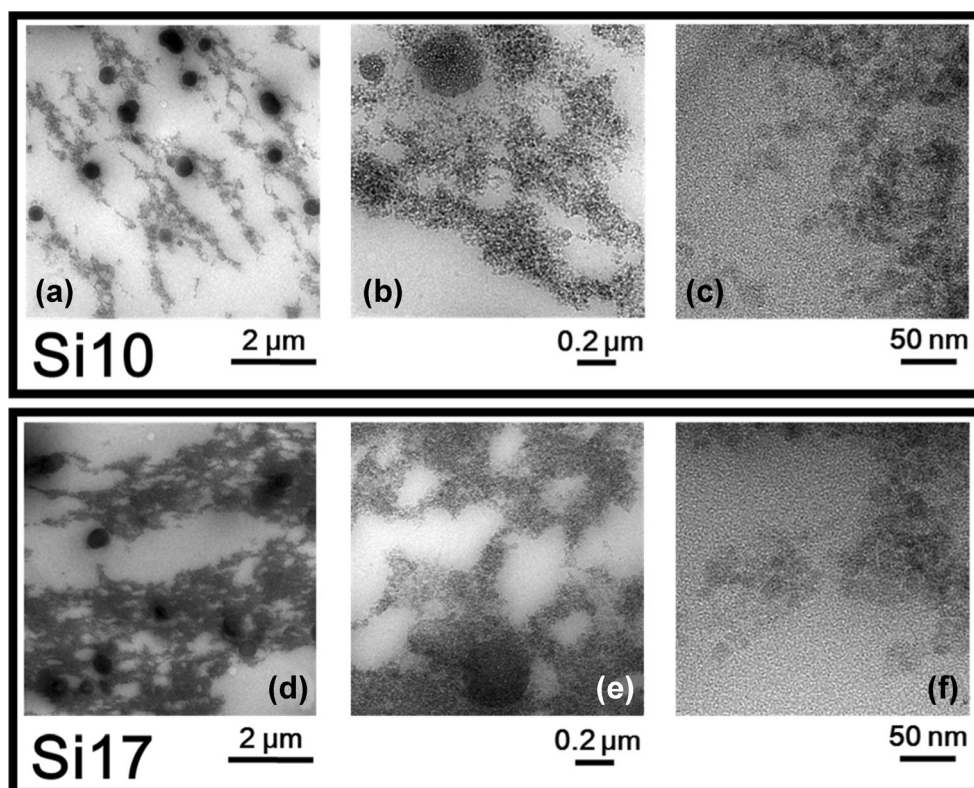
Morphological features of peroxide cross-linked in situ silica-filled nanocomposites as observed by TEM and SPM

Figure 2 shows TEM photographs of peroxide cross-linked in situ silica-filled nanocomposites with silica contents of 10 phr (Fig. 2a–c) and 17 phr (Fig. 2d–f). The dark parts in the micrographs show the in situ silica. It can be seen that a filler network structure was generated in both nanocomposites. A filler network of silica was detected more clearly in sample Si17, as was similarly observed in our previous work [19]. It should be pointed out in the present study that the formation of filler network in the rubber matrix is due to the processing technique, which NR particles were utilized as a template. In the high magnification images, i.e., Fig. 2c and f, individual in situ silica particles could be detected, and the particle size of the in situ silica was about 20 nm for both nanocomposites. Moreover, spherical aggregates with an average size of 500 nm were observed in both

nanocomposites. The generation of aggregates was ascribed to the presence of the surfactant, which was added to the latex when mixing with the peroxide cross-linking reagents before the sol–gel reaction. Namely, micelles were formed in the NR latex, and the TEOS and catalyst penetrated inside the micelles before the sol–gel reaction in the latex, which is opposite to the behavior reported in our previous papers [31, 32] and Miloskovska's paper [33], where inverse micelles were formed in the TEOS [32, 33].

In order to verify the characteristic of filler network more clearly, SPM observation of nanocomposites was carried out. Figure 3 shows phase images of films in situ silica nanocomposites: samples Si10 (upper images) and Si17 (lower images). In the phase images, bright and dark phases are attributed to hard and soft phases, which are silica and rubber phases, respectively. In the case of sample Si10, the filler network structure in rubber matrix was detected at magnification of $25 \mu\text{m}^2$ as shown in Fig. 3a. The observed filler network of in situ silica turns clearer by magnifying the interested area to $4 \mu\text{m}^2$ as shown in Fig. 3b. After magnifying the filler network, it was also observed that the in situ silica primary particles appear to be mutually fused to form their higher ordered structures, i.e., the aggregates, and/or the agglomerates. They were further clustered into a network in the rubber matrix. Additionally, it should be pointed out that the rubber phases, which were covered by in situ silica network, were so pure, as we can see no silica particles inside the network. Therefore, this morphological feature of model filler network is regarded to be very close to the ideal filler network structure.

Fig. 2 TEM photographs of in situ silica filled peroxide cross-linked nanocomposites



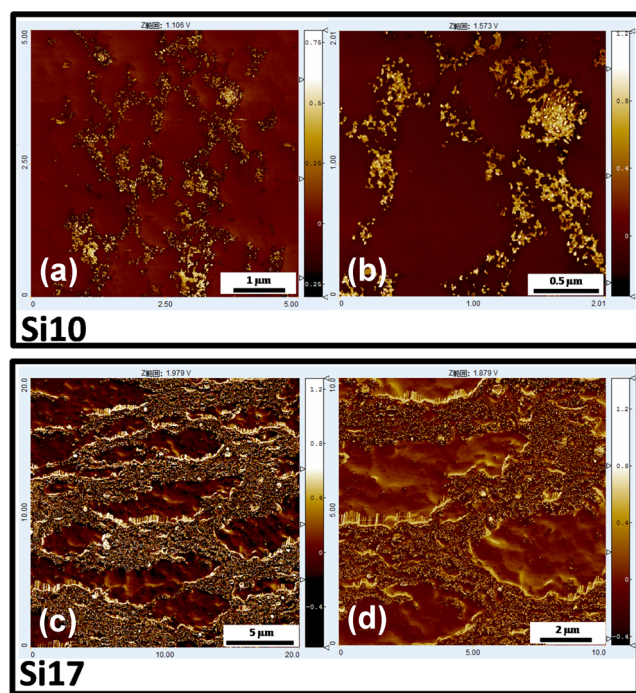


Fig. 3 SPM photographs of in situ silica filled peroxide cross-linked nanocomposites

Furthermore, it is noted that the spherical aggregates with an average size of 500 nm were also detected by SPM similarly with those observed by TEM.

In the case of sample Si17, a full range of filler network could not be observed at the same magnification, i.e., 25 μm^2 with that of samples Si10. The size of filler network of sample Si17 seems to be larger than that of sample Si10. Therefore, the magnification was decreased into 100 μm^2 as shown in Fig. 3d. At the magnification of 100 μm^2 , still it was difficult to see the full range of network structure in sample Si17. Therefore, the observation area was expanded to a larger size, i.e., 400 μm^2 , as shown in Fig. 3c. As a result, a full scale of filler network structure was detected. When comparing between the samples Si10 and Si17, some different characteristics of filler network was reasonably detected. The size of filler network in Si17 was larger and clearer than in sample Si10. When carefully checking SPM images, a little hard interface of rubber particles was observed inside the filler networks. On the basis of the size of NR particle (about 1 μm), therefore, the rubber phases seem to be consisting of a cluster of a few rubber particles. The clustering of rubber particles may be caused by destabilization of rubber particles during the sol–gel reaction at 40 °C for 5 h.

Tensile properties of peroxide cross-linked in situ silica-filled NR nanocomposites

Figure 4 shows the tensile stress–strain curves of the nanocomposites along with those of a peroxide cross-linked unfilled film prepared from NR latex using a similar procedure, except for the

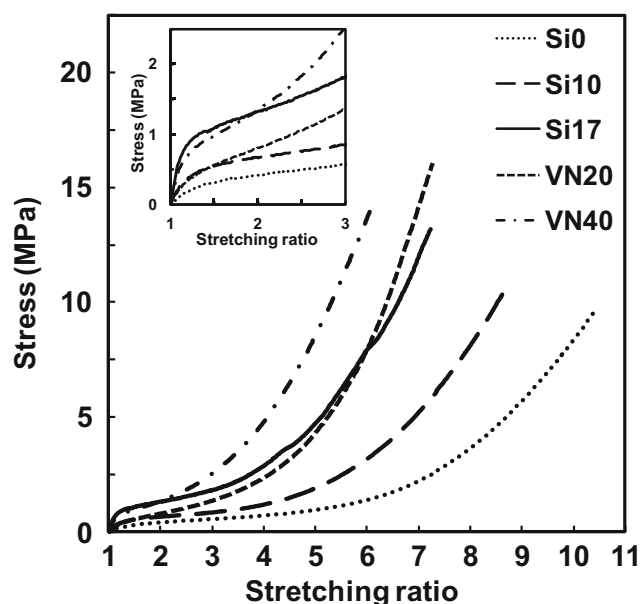


Fig. 4 Tensile stress–strain curves of peroxide cross-linked nanocomposites and unfilled film. The inset displays the tensile curves at low stretching ratio

sol–gel reaction of TEOS. Here, the stress–strain curves of two samples (VN20 and VN40) are also shown for comparison; these were prepared using a conventional mixing of commercial silica, VN-3, and a peroxide cross-linking of solid NR. It can be seen that, on comparing with the unfilled sample, a reinforcement by the silica clearly occurred in all the nanocomposites. Among the nanocomposites, sample VN40, which contained the highest amount of silica, exhibited the highest tensile stress for a stretching ratio around 2. Meanwhile, compared with the other nanocomposites, sample Si10, which contained 10 phr of in situ silica, showed the lowest tensile stress with a stretching ratio around 2.

However, as shown in the inset of Fig. 4, it is worth noting that the stress for a stretching ratio around 2 was a little higher in sample Si17 than in sample VN40, and was comparable between samples Si10 and VN20, although their silica contents were different. In general, stress in the initial stage of stretching is known to be related to the presence of filler aggregates and the filler network of a rubber matrix. Using three-dimensional electron transmission microscopy combined with tomography studying a conventional VN-3 silica filling of 40 phr in an NR matrix, one of the authors has reported observing the formation of silica filler networks in the peroxide cross-linked NR matrix [5, 6]. Therefore, the observed characteristics in the tensile properties of samples Si10 and Si17 clearly support the formation of a filler network in the nanocomposites, as shown in Figs. 2 and 3.

Dynamic mechanical properties of silica nanocomposites

Figure 5a–c shows the master curves of the dynamic mechanical properties constructed using horizontal shifting

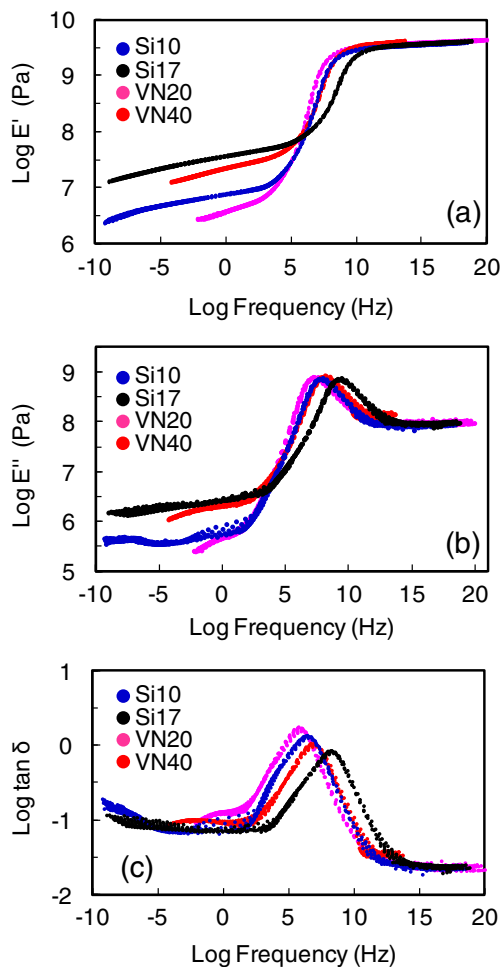


Fig. 5 Temperature–frequency dispersion of **a** storage modulus (E'), **b** loss modulus (E''), and **c** $\tan \delta$ of the nanocomposites

from the temperature–frequency dependence of the storage modulus (E'), loss modulus (E''), and $\tan \delta$ value of the nanocomposites, respectively. It can be seen in Fig. 5a and b that the dynamic moduli of the all nanocomposites in the high frequency region, i.e., log frequencies >12 Hz, are identical owing to an insufficient time for molecular relaxation of the NR molecules. However, the NR chains probably respond to the deformation by distorting their intermolecular distances. These distortions have a relatively high energy and thus result in a high modulus. This state is known to be a glassy region [34–36]. When the deformation time increased, i.e., at lower frequencies, i.e., $6 \text{ Hz} < \log \text{ frequencies} < 12 \text{ Hz}$, a reorientation and translation of the chain segments could occur more extensively, allowing the most severely distorted parts of the rubber chains to relax in a transition process. In this region, different characteristics among the nanocomposites were detected very clearly when plotting $\tan \delta$ against the logarithmic frequency scale, as seen in Fig. 5c. The details of the $\tan \delta$ results will be discussed later in this section.

Next to the transition region, for further decreases in frequency, i.e., log frequencies <6 Hz, the modulus of the all nanocomposites became very low, but the elongation and orientation of the chains was maintained. Especially in cross-linked rubber, the three-dimensional network structure works to prevent the conformational change; thus, a plateau region is generally observed [34–36]. In this study, the plateau region of the all nanocomposites was detected for log frequencies <4 Hz. Because of the different characteristics of the nanocomposites, variations in E' and E'' in the plateau region were distinguishable, as observed in Fig. 5a and b, respectively. The E' of nanocomposites are shown in Fig. 5a. It was found that E' in the plateau region, i.e., log frequencies <4 Hz, increased to higher values when the amounts of silica were higher, i.e., the E' of samples Si17 and VN40 were higher than that of samples Si10 and VN20, respectively. This tendency is generally observed as the restriction degree of rubber molecules can be higher when the higher filler content was used. Thus, this result clearly shows the presence of a good reinforcement effect of the both silica filling systems on the nanocomposites.

On the other hand, the effect of difference in the silica filling system on the E' in the plateau region can be evaluated by comparing between samples Si17 and VN20, which have similar contents of silica. It was clearly seen that E' in the plateau region of sample Si17 is much higher than that of sample VN20. This result suggests that a role of the filler network of the in situ silica brought a rigidity to the rubber matrix that considerably hindered the movement of rubber chains on deformation. On careful examination of E' for log frequencies <4 Hz, it was found that the rate of decrease in E' was slower in the in situ silica-filled samples than in the VN-3 silica-filled samples. In general, a decrease in E' in the low frequency region is ascribed to both a slippage of untrapped entanglements in the cross-linked network and to a molecular slippage associated with the disruption of pseudo-networks in the case of filled networks [34–38]. Consequently, in a system that has a higher degree of cross-linking or reinforcing, any disruption of the entanglements would be more difficult, thereby extending the plateau region of E' . The in situ silica network was presumed to provide an increase in stiffness to the nanocomposites compared with conventional silica. As a result, the decrease in E' was slower, and the plateau region was extended in the in situ silica-filled samples (Si10 and Si17) compared with the conventional silica-filled samples (VN20 and VN40).

This behavior became more pronounced when we considered the variation in E'' for log frequencies <4 Hz, as shown in Fig. 5b, where a similar tendency to that of E' was observed. In general, the degree of loss modulus is well known to depend on the degree of cross-linking. A lower degree of cross-linking results in a higher loss modulus because the possibility

of molecular slippages is higher in samples with a lower degree of cross-linking [37–39]. Subsequently, in the case of filled compounds, the loss modulus has been reported to increase with increasing filler content because of the higher potential to disrupt the filler networks [40–43]. As a result, the effect of increasing filler content on E'' can be seen very clearly in the plateau region. In fact, it was found in this study that E'' increased to higher values when the amounts of silica are higher, i.e., the E'' of samples Si17 and VN40 are higher than samples Si10 and VN20, respectively.

Similarly with the E' , the effect of silica filling system on the E'' in the plateau region can be evaluated by comparing between samples Si17 and VN20. It was clearly seen that E'' in the plateau region of Si17 is much higher and longer than that of VN20. This result can be ascribed to the disruption of the more rigid filler networks in the sample Si17 than in the sample VN20. It is also worth noting that the lower E'' value in the VN-3 nanocomposites may be attributable to the higher degree of filler–rubber interactions than the in situ silica nanocomposites. Higher filler–rubber interactions in the VN-3 samples are predicted from their dispersive morphology, as previously reported [5, 6], compared with the in situ silica networks observed in this study. Therefore, the higher filler–rubber interactions in the VN-3 samples may work like cross-linking points do and restrict the movement of rubber molecules. Thus, it is suggested that the high dissipation of E'' in the plateau region is mainly related to the morphology of the in situ silica-filled nanocomposites, which is of crucial importance for filled elastomers used for tire treads and the rolling resistance of tires [40–43].

In terms of the height of the $\tan \delta$ peak ($\tan \delta_{\max}$) as shown in Fig. 5c, it was observed that $\tan \delta_{\max}$ decreased with increasing silica content, i.e., samples VN40 and Si17 had lower $\tan \delta_{\max}$ than did VN20 and Si10, respectively. This result is in good agreement with that of E' as discussed above. Typically, the $\tan \delta$ peak has been reported to be influenced by several factors, for example, cross-linking degree, the fraction of filler and rubber, filler–rubber interactions, and the mobility of the rubber matrix [34, 35]. Therefore, the lower $\tan \delta_{\max}$ of the higher silica-filled samples can be explained by the lower mobility of the rubber matrix because of the presence of higher filler contents. Next, when comparing the two filling systems, it was also observed that the sample Si17 had a lower $\tan \delta_{\max}$ than did sample VN20. Similarly with the previous discussion on the effect of filler content on $\tan \delta_{\max}$, it can suggest that the lower $\tan \delta_{\max}$ of the in situ silica-filled samples can be explained by the lower mobility of the rubber matrix because of the presence of a filler network compared with the conventional silica samples.

Lastly, the $\tan \delta$ peaks of nanocomposites are considered as shown the results in Fig. 5c. It was found that $\tan \delta$ peaks shifted to higher frequencies when the amounts of silica are higher, i.e., $\tan \delta$ peaks of Si17 and VN40 were observed at the

higher frequencies than Si10 and VN20, respectively. In the case of VN-3 samples, where precipitated silica was used, it is well known that acidity due to the presence of silanol groups significantly affected on peroxide cross-linking [44]. As a result, when the higher VN-3 content was used in VN40, the lower cross-linking degree can be expected as suggested by the shift of $\tan \delta$ peaks to the higher frequencies compared to that of VN20. On the other hand, in the case of in situ silica samples, the lower cross-linking degree can be suggested to be due to the cross-linking activator, i.e., TEPA may work partially as a catalyst for sol–gel reaction before the cross-linking reaction was preceded. As a result, in sample Si17, the insufficiency of TEPA is supposed to be higher as the higher TEOS content was used for the sol–gel reaction. Consequently, the effect of insufficient amount of the catalyst in the in situ silica filled samples seems to be larger than that of acidity in the VN-3 silica. As a result, when comparing between the two systems, the in situ silica filled nanocomposites seem to have the lower cross-linking degree compared with conventional silica filled nanocomposites as suggested by the shift of $\tan \delta$ to the lower frequencies.

Until now, the characteristics of the dynamic mechanical properties have been discussed for systems comprising conventional filler mixed samples. However, it has been difficult for researchers to understand the role of the filler network in the system because conventional filler filled systems exhibit a large effect from various structures of filler aggregates in the rubber matrix. Our filler network structure of in situ silica in the nanocomposites, on the other hand, must minimize the effect of excessive filler aggregates in the rubber matrix. As expected, the filler network of the in situ silica shown in this study clearly shows the significant characteristics of the filler network in the dynamic mechanical properties, which may be the first such report, to the best of our knowledge.

Conclusions

In situ silica filling and peroxide cross-linking in NR latex was carried out to prepare a model nanocomposite to study the role of the filler network on the reinforcing. The suitable conditions of the peroxide cross-linking reaction were investigated to maintain an intrinsic morphology of the generated in situ silica in the NR latex, whereby a liquid state mixing method was utilized. The optimum conditions of peroxide cross-linking were determined from the viewpoints of network-chain density of the cross-linked films and the stability of the latex. The amount of *t*-BHP used and the cross-linking conditions employed were 1 phr and 80 °C for 0.5 h, respectively. A small amount of silane coupling agent, TEVS, was required to obtain homogeneous films. The filler network structure of in situ silica in the NR matrix was clearly observed using transmission electron microscopy and scanning probe

microscopy, even though the contents of in situ silica were only 10 and 17 phr. For comparison, conventional VN-3 silica-filled nanocomposites having silica contents of 20 and 40 phr were prepared and used as reference samples. The effect of the morphological features of the in situ silica and conventional silica-filled nanocomposites on the tensile and dynamic mechanical properties was clearly observed in this study.

Compared with the conventional VN-3 silica-filled nanocomposites, the unique and important aspects of the dynamic mechanical properties of the in situ silica-filled nanocomposites are the following: (1) higher E' and E'' values in the low frequency region, (2) longer plateau region of E' and E'' , (3) lower $\tan \delta_{\max}$, and (4) the shift in the $\tan \delta$ peak position at higher frequencies. The characteristics of points (1), (2), and (3) were mainly ascribed to the strong filler–filler interactions and that of point (4) was primarily caused by the lower filler–rubber interaction. Significant characteristics of the filler network of silica particles in the rubber matrix brought about these behaviors of in situ silica-filled nanocomposites.

Acknowledgments This work was partially supported by Kansai Research Foundation for technology promotion (project no. 2012R212).

References

- Bateman L (1963) The chemistry and physics of rubber-like substances. MacLaren & Sons, London
- Roberts AD (1988) Natural rubber science and technology. Oxford Science, Oxford
- Jones KP, Allen PW (1992) Historical development of the world rubber industry. In: Sethuraj MR, Mathew NM (eds) Developments in crop science, volume. 23, Natural rubber: Biology, cultivation and technology. Elsevier, Amsterdam, pp 1–22
- Rodgers B, Waddell W (2005) The science of rubber compounding. In: Mark JE, Erman B, Eirich FR (eds) The science and technology of rubber, 3rd edn. Elsevier Academic Press, Oxford
- Kato A, Ikeda Y, Kasahara Y, Shimanuki J, Suda T, Hasegawa T, Sawabe H, Kohjiya S (2008) Optical transparency and silica network structure in cross-linked natural rubber as revealed by spectroscopic and three-dimensional transmission electron microscopy techniques. *J Opt Soc Am B* 25:1602–1615
- Kato A, Kokubo Y, Tsushi R, Ikeda Y (2014) Hydrophobic and hydrophilic silica-filled cross-linked natural rubber: Structure and properties. In: Kohjiya S, Ikeda Y (eds) Chemistry, manufacture and applications of natural rubber. Woodhead Publishing, Elsevier, Oxford
- Mark JE, Pan SJ (1982) Reinforcement of poly(dimethylsiloxane) networks by in situ precipitation of silica: A new method for preparation of filled elastomers. *Makromol Chem Rapid Commun* 3: 681–685
- Yoshikai K, Yamaguchi M, Nishimura K (1996) Reinforcement of styrene-butadiene rubber by sol–gel process in the latex. *Nippon Gomu Kyokaishi* 69(7):485–490
- Yoshikai K, Ohsaki T, Furukawa M (2002) Silica reinforcement of synthetic diene rubbers by sol–gel process in the latex. *J Appl Polym Sci* 85:2053–2063
- Toutorski IA, Tkachenko TE, Maliavski NI (1998) Structural and chemical modification of polydiene latexes by gel derived silica. *J Sol–gel Sci Technol* 13:1057–1060
- Toutorski IA, Tkachenko TE, Pokidko BV, Maliavski NI, Sidorov VI (2003) Mechanical properties and structure of zinc-containing latex-silicate composites. *J Sol–gel Sci Technol* 26:505–509
- Tangpasuthadol V, Intasiri A, Nuntivanich D, Niyompanich N, Kiatkamjornwong S (2008) Silica-reinforced natural rubber prepared by the sol–gel process of ethoxysilanes in rubber latex. *J Appl Polym Sci* 109:424–433
- Poompradub S, Chaichua B, Kanchanaamporn C, Boosalee T, Prasassarakich P (2008) Synthesis of silica in natural rubber solution via sol–gel reaction. *Kautsch Gummi Kunstst* 408:152–155
- Chaichua B, Prasassarakich P, Poompradub S (2009) In situ silica reinforcement of natural rubber by sol–gel process via rubber solution. *J Sol–gel Sci Technol* 52:219–227
- Sirisamont J, Tangpasuthadol V, Intasiri A, Na-Ranong N, Kiatkamjornwong S (2009) Sol–gel process of alkyltriethoxysilane in latex for alkylated silica formation in natural rubber. *Polym Eng Sci* 49:1099–1106
- Satraphana P, Intasiri A, Tangpasuthadol V, Kiatkamjornwong S (2009) Effects of methyl methacrylate grafting and in situ silica particle formation on the morphology and mechanical properties of natural rubber composite films. *Polym Adv Technol* 20:473–486
- Watcharakul N, Poompradub S, Prasassarakich P (2011) In situ silica reinforcement of methyl methacrylate grafted natural rubber by sol–gel process. *J Sol–gel Sci Technol* 58:407–418
- Scotti R, Wahba L, Crippa M, D’Arienzo M, Donetti R, Santo N, Morazzoni F (2012) Rubber–silica nanocomposites obtained by in situ sol–gel method: Particle shape influence on the filler–filler and filler–rubber interactions. *Soft Matter* 8:2131–2143
- Tohsan A, Phinyocheep P, Kittipoom S, Pattanasiriwisawa W, Ikeda Y (2012) Novel biphasic structured composite prepared by in situ silica filling in natural rubber latex. *Polym Adv Technol* 23(10): 1335–1342
- Tohsan A, Ikeda Y (2014) Generating particulate silica fillers in situ to improve the mechanical properties of natural rubber. In: Kohjiya S, Ikeda Y (eds) Chemistry, manufacture and applications of natural rubber. Woodhead Publishing, Elsevier, Oxford
- Poompradub S, Thirakulrati M, Prasassarakich P (2014) In situ generated silica in natural rubber latex via the sol–gel technique and properties of the silica rubber composites. *Mater Chem Phys* 144(1–2):122–131
- Ikeda Y, Tohsan A (2014) Stepwise strain-induced crystallization of biphasic-structured soft composites prepared from natural rubber latex and silica generated in situ. *Colloid Polym Sci* 292:567–577
- Ikeda Y, Higahsitani N, Hijikata K, Kokubo Y, Morita Y, Shibayama M, Osaka N, Suzuki T, Endo H, Kohjiya S (2009) Vulcanization: New focus on a traditional technology by small-angle neutron scattering. *Macromolecules* 42(7):2741–2748
- Yasuda Y, Minoda S, Ohashi T, Yokohama H, Ikeda Y (2014) Two-phase network formation in sulfur cross-linking reaction of isoprene rubber. *Macromol Chem Phys* 215:971–977
- Williams ML, Landel RF, Ferry JD (1955) The temperature dependence of relaxation mechanisms in amorphous polymers and other glass-forming liquids. *J Am Chem Soc* 77(14):3701–3707
- Treloar LRG (1975) The physics of rubber elasticity. Clarendon, Oxford
- Class JB, (2002) Fundamentals of peroxide cure of elastomers. Paper No.B, ACS Rubber Div. Meeting, Georgia
- Ashizawa T (1963) Lecture of latex technology. *Gomu* 10(1):29–36
- Dufresne ER, Stark DJ, Greenblatt NA, Cheng JX, Hutchinson JW, Mahadevan L, Weitz DA (2006) Dynamics of fracture in drying suspensions. *Langmuir* 22(17):7144–7147
- Tirumkudulu MS, Russel WB (2005) Cracking in drying latex films. *Langmuir* 21(11):4938–4948

31. Poompradub S, Kohjiya S, Ikeda Y (2005) Natural rubber/in situ silica nanocomposite of a high silica content. *Chem Lett* 34(5):672–673
32. Ikeda Y, Poompradub S, Morita Y, Kohjiya S (2008) Preparation of high performance nanocomposite elastomer: Effect of reaction conditions on in situ silica generation of high content in natural rubber. *J Sol–gel Sci Technol* 45(3):299–306
33. Miloskovska E, Hansen MR, Friedrich C, Hristova-Bogaerds D, Duin MV, With G (2014) In situ silica nanoparticle formation in a rubber matrix monitored via real-time SAXS and solid-state NMR spectroscopy. *Macromolecules* 47(15):5174–5185
34. Ferry JD (1980) *Viscoelastic properties of polymers*, 3rd edn. Wiley, Ontario
35. Kramer O, Hvidt S, Ferry JD (1994) Dynamic mechanical properties. In: Mark JE, Erman B, Eirich FR (eds) *Science and technology of rubber*, 2nd edn. Academic, London
36. MacKnight WJ, Shaw MT (2005) (eds) *Introduction to polymer viscoelasticity*, 3rd edn. Wiley, New Jersey
37. Ferry JD, Mancke RG, Maekawa E, Ōyanagi Y, Dickie RA (1964) Dynamic mechanical properties of cross-linked rubbers. I. Effects of cross-link spacing in natural rubber. *J Phys Chem* 68(11):3414–3418
38. Ferry JD, Langley NR (1968) Dynamic mechanical properties of cross-linked rubbers. VI. Poly(dimethylsiloxane) networks. *Macromolecules* 1(4):353–358
39. Saphiannikova M, Toshchevikov V, Gazuz I, Petry F, Westermann S, Heinrich G (2014) Multiscale approach to dynamic-mechanical analysis of unfilled rubbers. *Macromolecules* 47(14):4813–4823
40. Meera AP, Said S, Grohens Y, Thomas S (2009) Nonlinear viscoelastic behavior of silica-filled natural rubber nanocomposites. *J Phys Chem C* 113:17997–18002
41. Mujtaba A, Keller M, Ilisch S, Radusch HJ, Thurn-Albrecht T, Saalwächter K, Beiner M (2012) Mechanical properties and cross-link density of styrene–butadiene model composites containing fillers with bimodal particle size distribution. *Macromolecules* 45(16):6504–6515
42. Medalia AI (1978) Effect of carbon black on dynamic properties of rubber vulcanizates. *Rubber Chem Technol* 51:437–523
43. Wang MJ (1998) Effect of polymer-filler and filler–filler interactions on dynamic properties of filled vulcanizates. *Rubber Chem Technol* 71:520–589
44. Wanger MP (1976) Reinforcing silicas and silicates. *Rubber Chem Technol* 76:703–774